IEEE Access
Multidisciplinary ⋮ Rapid Review ⋮ Open Access Journal

Received 26 May 2024, accepted 17 June 2024, date of publication 21 June 2024, date of current version 5 July 2024.

Digital Object Identifier 10.1109/ACCESS.2024.3417377

RESEARCH ARTICLE

Vibration Signal Based Abnormal Gait Detection and Recognition

JUANJUAN CHEN[1], CHENGLIANG WANG[2], (Member, IEEE), AND YILUO LIU[3]
[1]School of Computer and Information Science, Chongqing Normal University, Chongqing 400023, China
[2]College of Computer Science, Chongqing University, Chongqing 400023, China
[3]School of Computer Science, Chongqing University, Chongqing 400023, China

Corresponding author: Juanjuan Chen (20131036@cqnu.edu.cn)

This work was supported by Chongqing Natural Science Foundation Innovation and Development Joint Fund under Grant CSTB2023NSCQ-LZX0109.

ABSTRACT Experts have been researching different types of gait since the 19-century. The way people walk can give a myriad of clues as to the health of a person. Abnormal gait detection might help protect senior people from injury and reveal underlying health problem. In aging societies, the application of recognition of abnormal gait based on vibration signal is very useful, especially for those people who live by them own. Unlike other methods in the related research requiring image acquisition equipment and wearable device to identify relevant feature information, not even mention many are intrusive or too complicated for users. The proposed systematic prototype firstly uses foot vibration signals as the source for abnormal gait and fall detection. This paper investigates algorithmic aspects; the particular algorithm's framework involves gathering data from several artificial sensors. An altered version of the Dynamic Time Warping (DTW) algorithm computes the anomaly index after splitting the active portion into active elements and denoising the active elements. Next, the K-Nearest Neighbor (KNN) algorithm separates the anomaly indices into distinct groups and generates the projected values representing the user's gait. Ultimately, the predicted values are processed by the Hidden Markov Model (HMM), which then determines the user's gait. In the meantime, if an abnormality of gait arises for various experimental environments, subjects, and shoe types, etc., its corresponding index and the value representing the user's gait will also change in comparison to his or her normal gait, which will remain unaffected by the environment and the shoe type of the subject. As a result, the experiments in this paper are flexible. In the experiments, various sensor placements and subjects can also, to the greatest extent possible, reflect the algorithm's adaptability to these changes.

INDEX TERMS Abnormal gait, dynamic time warping (DTW), hidden Markov model (HMM), vibration signal.

I. INTRODUCTION

Internet of Things (IOT) has many potential applications and can be implemented in fields of smart homes, offering important features like identification recognition, sleep sensor, and fall protection etc. Moreover, this technology has tremendous application value in abnormal activity detection for older generation. China's seventh national census revealed that the proportion of the country's population over 60 years old rose to 264 million, or 18.7% of the total. By 2027, this percentage is anticipated to increase to 20% [1]. The world is currently seeing an aging trend, not just China. The United Nations released the World Social Report 2023 on January 12, 2023, which states that by mid-century, there would be 1.6 billion people worldwide who are 65 years of age or older. The number of individuals who are 80 years of age or older is predicted to increase much more quickly [2]. The trend requires spending more social resources in medical care to maintain the living quality of aging people. However, it is unrealistic to rely on more human resources under the context of working force shortage. Scientific aids and technology will help solve the problem in large scale.

The associate editor coordinating the review of this manuscript and approving it for publication was Zihuai Lin.

Recognizing the limitations imposed by societal and human resources emphasizes how urgent it is to look for scientific solutions to the problems an aging population presents. Among existing options, one important area of focus is the recognition of aberrant gait. The recognition of abnormal gait based on vibration signal is very useful to protect seniors from injury by revealing underlying health problems and timely informing caregivers. The way people walk can give a myriad of clues of health, as abnormal gaits are early signs of disease. The gait pattern of a hemiplegic patient, for example, is different from that of people without disabilities in terms of movement pace, rhythm, symmetry and walking speed. Hence early disease detection and proper treatment can improve the quality of life for seniors.

Fall is one of the major issues which can endanger the lives of older people. According to [3], fall detection system helps solitary seniors with immediate medical care and support once a fall event happens. A well functioned fall detection system may reduce 80% of death risks and helps seniors live as long as possible. Numerous research studies investigate the use of wearable technologies, computer vision, sonar technology and radio frequency technologies to detect falls in everyday environment. Although wearable sensor provides accuracy and sensitivity for fall detection, it is not convenient as seniors wear sensors or tags everywhere [4]. Vision-based fall detection system operates by analyzing real-time movement with the fall-event judging criteria. However, computer vision technologies function best in confined space with good illumination and less obstacles. Moreover, vision-based technology violates people's privacy, hence it is not applicable for large scale. Likewise, there are disadvantages of radio frequency technology. First, the costs for massive distribution of sensors outweigh the possible benefits [5]. Second, fall could not be detected by radio frequency technology before it really happens. Sound technology can detect fall in despite of background noises, still the environmental sound level has great impact on the accuracy of the audio system [6], especially in places nearby noise pollution source of rail station or highway.

This paper introduces vibration signals to monitor and detect continuously floor vibrations produced by daily activities. Compared with the detection technologies mentioned above, the advantages are: firstly vibration is unaffected by environmental noise or space obstruction. Secondly there is no need to deploy massive sensors across place. Lastly people do not need to wear any devices with them. Encouragingly, the smart living system based on vibration can be built in IOT environment [7].

In our prototype, walking vibration and fall pattern are recorded to compose activity element sequences. Based on the analysis of sequences, our prototype may surmise whether fall event or abnormal gait occur. There are three major issues to be addressed in our research.

(1) **gait diversity**: Many diseases affect gait and lead to walking patterns different from normal ones. In order to solve the problem of abnormal gait detection, we adopt DTW-KNN framework. Instead of applying general gait standard, the framework detects abnormal gait by comparison with personal normal gait in different walking patterns.
(2) **environmental interference**: Unusual activity elements as a result of environmental interference do not necessarily mean walking abnormality; thereof this paper focuses on identifying abnormal gait with certain interference in various settings. In this prototype, we adopt HMM algorithm to increase the accurateness and robustness to identify abnormal or irregular strides, in particular in settings with interference.
(3) **rapid setup**: The gait diversities may cause the problem that fixed training dataset and results are not adaptable to various situations. Our prototype is aimed to collect field data at a fast pace and train limited number of activity elements to realize functionality.

This research discusses vibration based gait identification as non-wearable fall detection solution in settings with interference. Specifically, we updated the computing methods of DTW algorithm by changing the Euclidean distance to the Centre distance. The method of Segment Comparison is applied to compare activity elements. Furthermore, to evaluate the generality of our approach, we also apply it to the setting with interference. The proposed methods are carefully evaluated and the results show promising outcomes. The structure of this paper is as follows. After related works in part 2, related problems and the system design of each module are addressed in part 3. Experimental results are discussed in part 4 and the conclusion was given in the final part.

II. RELATED WORKS

There are many researches about gait recognition, in which computer vision based and wearable devices based gait recognition approaches are mostly common. Researches about vibration based gait recognition are less studied, mainly focusing on human identification and very few on abnormal gait recognition.

By using image technology to process data collected by 2D or 3D devices, computer vision technique is able to analyze gait sequence. Yao et al. [8] proposed a novel model of Skeleton Gait Energy Image (SGEI) based on the robust skeleton points produced from a two-branch multi-stage CNN network, which has been presented increased robustness for gait recognition. Babaee et al. [9] proposed a gait recognition algorithm from an incomplete gait cycle information by creating an incomplete Energy Image (GEI) from a few available silhouettes of a subject and reconstructing the complete GEI from incomplete GEI using a deep auto-encoder. Nguyen et al. [10] created a model based on human joint positions (Kinect skeleton), which shows that very promising in distinguishing normal and abnormal gaits. Zhang et al. [11] employed K-means to cluster all gait features obtained from a number of walking

videos into 6 key gait features, and three Support Vector Machines (SVMs) are trained for walking pattern detection. Liao et al. [12] proposed a model of pose-based temporal-spatial network (PTSN) for gait recognition by using Long Short Term Memory (LSTM) to analyze time sequence feature. However, this gait recognition method imposes high demands on environmental conditions, lighting variations, shooting angles among others. It relies on camera equipment for capturing and transmitting image data. Consequently, recognition is significantly influenced by camera positioning and angle. Therefore, these methods raise numerous privacy concerns.

Wearable sensors technology integrates Data Acquisition Unit into common objects that users carry with them, such as smart phone or shoe pad. Ronao et al. [13] proposed a two-stage continuous hidden Markov model (CHMM) approach for the task of human activity recognition using accelerometer and gyroscope sensory data gathered from a smartphone. Segundo et al. [14] analyzed and proposed a Human Activity Recognition (HAR) system based on Hidden Markov Model that uses accelerometer signals from different smartwatches and smartphones to identify six different human gaits, walking, running, standing, sitting, walking upstairs and walking downstairs. Wang et al. [5] presented gait assessment system based on SVM (support vector machine) classifier and on gait variability-based features calculated from the hip and knee joint angle trajectories recorded using wearable IMUs, to distinguish healthy gait patterns from the pathological ones. Lin et al. [15] designed Smart Insole integrated with pressure sensors covering 80% of plantar to fully measure the pressure, offering precise acquisition of gait information and providing an unobtrusive way to perform the gait monitoring. But these works of gait recognition require the user to wear a specific device at all times, reducing user comfort and increasing the risk of older user forgetting to wear it or wearing it incorrectly, which would render the entire detection system ineffective because it would not be able to obtain the correct data.

Using the Method of Characteristics to identify Step Event and calculating eigenvalue, vibration signal based technique identifies gait modes by classifying eigenvalue into different groups. Dong et al. [16] introduced an indoor person identification system that utilizes footstep induced structural vibration. By sensing floor vibration and detects the footstep signal, the system extracts features from the signals that represent characteristics of each person's gait pattern. Clemente et al. [17] presented a smarter fall detection system that uses floor seismic data produced by footsteps and introduced a voting system among sensor nodes to improve accuracy in person identification. The vibration signal solves the problem caused by abnormal gait recognition based on computer vision and wearable technology. These methods requires extensive computing resources, making them difficult to implement in home settings, particularly for elderly residents.

Addressing the limitations in prior studies, this paper introduces a vibration-signal-based method for recognizing abnormal gaits, characterized by its high accuracy and robustness in detecting both abnormal gait and fall events.

III. SYSTEM DESIGN

A. RESEARCH STRATEGY

As people have different gait modes, the problem of using the Method of Characteristics to detect abnormal gait is that it is difficult to find suitable eigenvalue to describe various gait modes. The signal before denoising in Fig. 1 is represented by a1 and the signal after denoising by a2. The denoised signal is much more readable and suitable for additional investigation, as can be observed. Furthermore, the active element waveforms of the two gaits in groups B and C differ significantly from one another. Group b represents a regular user, and group c is a simulated hemiplegic user: As for group b, there are two clear peaks in every activity element, separated by a purple dashed line in a2 and b3, and the first peak is highlighted by red square and the second by green. c1 and c3 in group c are similar with group b, and in group c the first peak is highlighted by purple square and the second by orange square. However, the orange square in c2 and c4 show a period of small fluctuations that alternate with smaller peaks. From figure 1 it may conclude that there are regularity and similarity of activity elements in one type of gait mode, and yet there are obvious difference between various gait modes. Based on the characteristics, this research adopts the DTW algorithm to compare similarity among active elements. Each element is compared with two elements before it to calculate the abnormal index of difference and compose the abnormal index pair. Next KNN algorithm is applied identify whether the active element represents abnormal gait or any predicted value of certain situation.

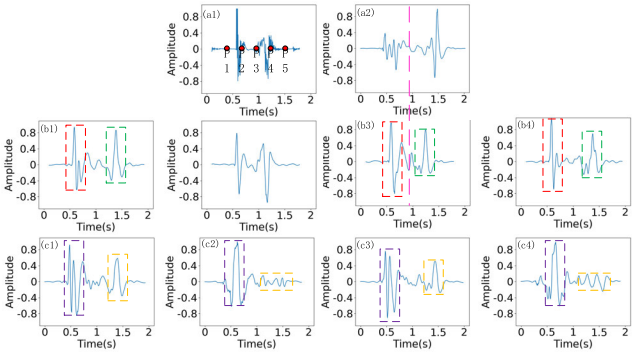

FIGURE 1. Sketch map of active elements.

Environmental interference issue, such as stepping on loose floor, might cause active element of normal gait to be classified to abnormal gait. Hence using the predicted value of single active element to identify gait mode will cause recognition error [17], [18]. However, this interference only has impact on the present active element and not on the successive elements. Therefore, integrating neighbor

active elements as a whole complex is a way to correct the gait recognition result caused by environmental interference issue.

In order to solve these problems, this research adopts HMM as the method to recognize gait mode. DTW-KNN algorithm produces the sequence of predicted values of active elements, named predicted sequence. HMM algorithm calculates the predicted complex number to produce the gait mode with the maximum probability, hence correcting the gait recognition deviation caused by interfered active element in most cases.

Besides gait diversity and environmental interference issues, there are three more issues to be addressed to solve the problem of abnormal gait recognition based on vibration signal.

The first question is the noise issue. All collected data contains certain level of noise, which could be produced by construction shaking, or electric appliances working. As background noise effects active elements, so this paper adopts the Wavelet Transform Denoising Algorithm to eliminate background noise.

The second issue is related with active element separation. In practice, the major part of collected data is background noise, and only a small part is active elements that need segmentation and storage. So far, available segmentation methods can only identify the start of active element, and can hardly identify the end of it. Moreover, segmenting active element by defining the threshold value performs not well because of background noise interference. So in this paper we design a method based on the Second-Moment Method to identify and divide active elements.

The last issue is about the active element selection. When multiple sensors coordinate together, various sensor data collected might be inconsistent, so it is necessary to select the optimal active elements. This paper also develops an optimizing algorithm to solve this problem, explained later.

B. SYSTEM FRAMEWORK

The prototype contains four modules, including Data Sampling Module, Denoising Module, Predicting Module and Decision Module. Fig. 2 describes the relationships among those modules and the components in them. The hardware part of this system is made up of sensor units, which interact through WiFi network. The second moment method serves as the foundation for the segmentation and optimization techniques employed in the data sampling module. This study allocates some of the center node's tasks to the edge nodes and coordinates the dispersed working sensors to minimize the load of data transmission and increase the detection range, in addition to designing the active element segmentation method to store the data more efficiently. This is due to the fact that the majority of redundant data is present in the collected data, and retaining all the data will strain the device and consume storage capacity. A seismic detector, an amplifier, and a BeagleBone development board make up the hardware used for data acquisition. The BeagleBone development board, which is the most important component of the system, is a low-cost, low-performance, on-board Linux system, programmable embedded development board, around which the entire system is built. The wavelet thresholding method is applied in the Denoising Module to eliminate background noise and enhance the signal to noise ratio. The Predicting Module is a architecture of DTW-KNN framework. DTW calculates abnormal index of active element, and then KNN classifies and produces the predicted value of the active element. The Decision Module uses HMM to analyze predicted sequence to identify gait mode.

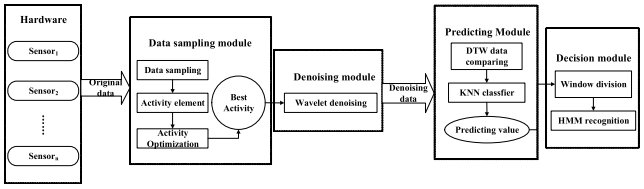

FIGURE 2. System framework.

C. HARDWARE SENSORS

The hardware for collecting vibration data includes: sensor unit as edge node and personal computer as center node. As indicated from fig.3, every edge node is composed by three major parts, i.e. seismometer, amplifier and Beagle Bone development board. The seismometer detects vibration signal with 200Hz sampling frequency, while the amplifier amplifies the original sample signal by enhancing the ratio of signal to noise. The Beagle Bone development board is the single chip computer embedded with Linux system, which operates various processing programs. BeagleBone is a powerful, low-cost, open-source Linux computing platform with processor speeds of up to 2 billion instructions per second, providing users with ample computing power for a variety of complex tasks. Compared to other similar products, the cost of the BeagleBone is lower, usually between \$45∼\$55, which makes it ideal for prototyping and product development. It provides standard interfaces for many electronic devices for easy connection to other hardware components, modules, and USB devices. At the same time, the BeagleBone has low power consumption, with a power consumption of only about 1 watt (when idle) and a maximum peak power consumption of only 2.3 watts, which helps to save energy and extend battery life. By using daughter boards and USB devices, users can easily expand the functions and interfaces of the BeagleBone to meet the needs of different application scenarios. In addition, BeagleBone has a large number of innovator and enthusiast forums where users can share experiences, exchange questions, and get technical support and guidance. As open-source hardware, BeagleBone supports open-source software tools and applications, providing users with greater flexibility and freedom. When equipping edge node, seismometer is fixed by wax oil to the floor to better collect the high frequency vibration signal [19].

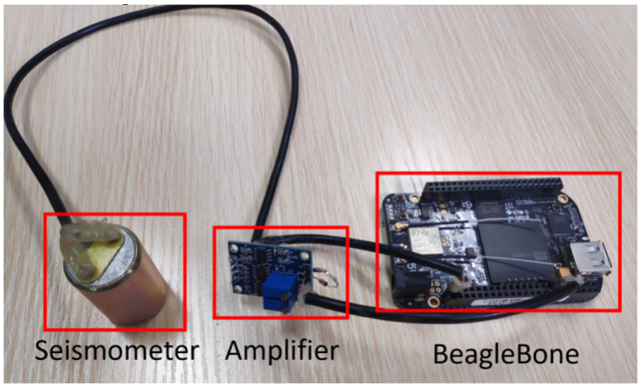

FIGURE 3. Edge node composition.

D. DATA ACQUISITION MODULE

1) ACTIVE ELEMENT SEPARATION

$S_n = \{x_1, x_2, x_3, \cdots, x_{n-1}, x_n\}$ indicates the sample sequence, $x_i (1 \leq i \leq n)$ refers to the sample value at time i. Here the range of sample value is set as $0 \leq x_i \leq 1.8$.

The active element is the valid part in a sample sequence, i.e. the sub-sequence contains user's activity data. This research adopts the second-moment method to calculate separation point p, which satisfies the following conditions:

$$m_2 = \frac{1}{N} \sum_{i=p}^{p+N} (x_i - \mu)^2 \geq \delta \tag{1}$$

N indicates the size of time window, $\mu = \frac{1}{N} \sum_{i=p}^{p+N} x_i$. This paper chooses 100 millisecond as the window size, which contains 20 sample values ($N = 20$), to calculate separation point of active element. In this paper, considering the computing power of the BeagleBone edge device and the gait characteristics of the elderly in the room, 100ms is selected as the window size, which mainly captures the effective vibration signal in the complete footsteps of the elderly, rather than capturing the whole process. When $m_2 > \delta$ (δ is the threshold), then this point is determined as a separation point. Here the threshold is set as three times of the standard deviation of background noise, i.e. for a sampling sequence of background noise without active element, $S_m = \{y_1, y_2, y_3, \cdots, y_{m-1}, y_m\}$, the threshold value δ is given as:

$$\delta = \varepsilon \sqrt{\frac{\sum_{i=1}^{m} (y_i - \bar{y})^2}{m - 1}} \tag{2}$$

$\bar{y}$ is the sample mean, and ε refers to threshold factor, here $\varepsilon = 3$. The louder is the accidental noise in background, the greater value of ε will be. After calculation, this paper has a sequence of separation points, given as $P_s = \{p_1, p_2, p_3, \cdots, p_{s-1}, p_s\}$. $p_j (1 \leq j \leq s)$ indicates the value of the jth separation point, shown in Fig.1(a1). Here only p_1 and p_5 are necessary in the sequence $p_1 \sim p_5$ for separating active element. So these two are effective points and $p_2 \sim p_4$ are redundant points. An effective point p_j satisfied the follows:

$$p_{j+1} - p_j \geq \gamma N, 2 \leq j < j + 1 \leq s - 1$$

γ is the separation factor, and here $\gamma = 3$. Moreover, the first point p_1 and the final p_s are always effective. Then this paper has P_t as sequence composed by effective points, and every two points may separate an active element A_i, defined as follows:

$$\begin{aligned} A_i &= S_{p_{2i-1}, p_{2i}} \\ &= \left\{x_{p_{2i-1}}, x_{p_{2i-1}+1}, x_{p_{2i-1}+2}, \cdots, x_{p_{2i}-1}, x_{p_{2i}}\right\}, \\ &\quad p \in P_t, 1 \leq i \leq \frac{t}{2} \end{aligned}$$

Moreover, one active element is inadequate to test which edge node produce the best element, hence the amount of signal energy is considered to make decision. This research adopts Fast Fourier Transform (FFT) to calculate amount of energy by converting active element from time domain to frequency domain. As amount of energy reflects in general the intensity of a signal, so the energy level E_i of element A_i is given as:

$$E_i = \sum |x_l|^2, x_l \in COFFT(A_i) \tag{3}$$

$COFFT(A_i)$ indicates the coefficient of of A_i in FFT calculation. The edge nodes will upload a two-tuple $AE_i = (A_i, E_i)$ to center node, where the active element selection will be processed next.

2) ACTIVE ELEMENT SELECTION

The algorithm in this research is developed on Network Time Protocol (NTP), and all edge node synchronizes with the central node through NTP. A data storage is created for every edge node in the central node. When active element is separated in the edge node, data consisting of the element and its energy is sent to the central node. Then by comparing the energy of different active elements sent by all edge nodes at this time, the element with the maximal energy will be selected and saved. The process is shown in Algorithm 1.

Algorithm 1 Active Element Selection

Input: sensor socket list *sl*
Output: NULL(put the best signal bss into a queue *oq*)
1: **for** *c* in *sl*:
2: create queue sq_i = NULL; //create active element storage queue
3: **while** not END:
4: wait until get a new signal ns_i;
5: **if** sq_i is NULL:
6: sq_i.put(nsi); //
7: **else**:
8: *bss* = NULL;
9: **for** each sq_i:
10: **if** sq_i is not empyt:
11: $js_i = sq_i$.get();
12: *bss* = maxEnergy(*bss*, js_i); //choose larger value from *bss and* js_i
13: *oq*.put(*bss*);
14: sq_i.put(ns_i)
15: **return** NULL

In this algorithm, the input is connected sensor socket list sl, and every element in the list is a socket object from which data will be obtained from sensors. Filtered signal is then written to a queue, waiting to be called at the next step. The 1st and 2nd line refer to the data storage queue for every element from the linked list. The 3rd line refers to program ends once receiving ending signal. The 4th line indicates waiting until getting a new signal sent by edge node. The 5th and 6th line refer to store data when the data queue that matching an active element is empty, which may happen just after the former active element is processed. Line 8th to 14th indicate the steps to process active element. From all data queues which are not empty, the element with the maximal energy is selected and stored in the signal queue, and then this active element received is stored in the corresponding sensor queue.

E. DENOISING MODULE

Since the correlation and modal maxima denoising algorithms are best suited for denoising signals with high and low signal-to-noise ratios, respectively, they require a lot of computational power and high arithmetic complexity when used on embedded platforms with low performance. For this reason, this paper uses the most popular algorithm, the wavelet threshold denoising algorithm, to automatically remove background noise.

Choosing the threshold or threshold function and how to handle the wavelet coefficients are crucial steps in the wavelet threshold denoising process that control the denoising impact. Hard and soft threshold functions are the most widely used types of threshold functions. Nevertheless, there may be disadvantages to any of the approaches. The soft threshold function will always be different from the existence of the difference when the conditions are met, which will result in the reconstruction of the signal and the real signal deviation between the signal. The hard threshold is discontinuous throughout the entire wavelet domain and has breakpoints in the position, so the original signal after hard threshold denoising may appear obvious oscillations after reconstruction.

In this work, the improved threshold function and Equation 4 are used to solve the shortcomings of the soft and hard threshold functions:

$$W'_{j,k} = \begin{cases} W_{j,k} - \dfrac{2\lambda}{1+\exp\left(\lambda - W_{j,k}\right)} & W_{j,k} \geq \lambda \\ 0 & \left|W_{j,k}\right| < \lambda \\ W_{j,k} + \dfrac{2\lambda}{1+\exp\left(\lambda + W_{j,k}\right)} & W_{j,k} \leq -\lambda \end{cases} \tag{4}$$

Compared to the soft threshold function, the improved function exhibits a steadily decreasing deviation as it moves towards infinity. The function can also meet the similar trend of maintaining the signal coefficients across the wavelet domain while weakening the noise coefficients. The function continues to be continuous as the wavelet coefficients converge to zero.

As seen in Fig. 1 (b2), the signal noise is decreased following the denoising process.

F. PREDICTING MODULE

The Predicting Module is built with DTW-KNN framework. Here this paper improves DTW algorithm from two aspects to adapt active element comparison. Firstly this paper changes Euclidean Distance to Center distance; secondly it adopts Segment comparison. The distance function in DTW is defined the Centre distance, given as $f\ (x_i, y_i) = ||x_i| - |y_i||\circ$

When performing comparison, the active element is adjusted to X axis, and the absolute values of x_i and y_i indicate the distance of sampling element to X axis. Some part of active element might be symmetrical to X axis, such as parts shown in the green box in Fig. 1 (b2). In essence, those parts are same kind of vibrations. The greater abnormal index produced by Euclidean distance will affect the inference value, so it is more reliable to use the Center distance instead.

As stretching and squeezing of active element in DTW calculation will cause its feature hardly being reflected in frequency domain, hence the index difference between active element and abnormal element will be not significant enough. According to literature [20], Gait mode describes the way of walking and four limbs movement characteristics. A gait starts from one heel touches the ground and ends when the toe leaves the ground. During the whole process, a series of muscles stretch and contract. First the ankle dorsiflexion stretches, then the gastrocnemius and soleus muscle stretch, finally the gastrocnemius and soleus muscle contract. This process indicates multiple smaller stages can be divided in one active element. According to the analysis, the active element could be divided into several smaller parts to calculate separately with DTW algorithm, and then added together. The active element division is indicated in Fig. 1 (a2) and (b3). (b3) is a normal active element and (a2) is abnormal. Both elements are divided by pink dot line and compare both left and right side to improve the classification accuracy.

Abnormal index generated by DTW calculation is input into KNN classifier, producing the predicted value of active element. As the predicted value relates to user's gait only and indicates the gait variation, so predicted sequence composed by those values can be used in HMM Decision Module to recognize gait.

G. DECISION MODULE

$\lambda = (N, M, \pi, A, B)$ is the HMM with five elements, or $\lambda = (\pi, A, B)$ in short. N is the infinite set of states and M is the infinite set of observations. π is the probability distribution of initial state, and A is the state transition matrix. B is the observation probability distribution matrix, i.e. the confusion matrix. The parameter set $\lambda = (\pi, A, B)$ is trained with Baum–Welch algorithm. According to the observed sequence, Viterbi algorithm is applied then to find out the best hidden state sequence which most likely produces the observed sequence. The HMM is defined as follows.

1) STATE SET

The hidden state is not directly observed in HMM decoding process, hence it is a finite set to be solved. In our research domain, the hidden state indicates user's gait mode, i.e. normal, abnormal and fall, which cannot be obtained from the predicted sequence. The three states are all status in the state set in our research.

2) OBSERVATION SET

Observation set is an important known condition to solve the hidden state, in which every hidden state has a certain probability to produce possible observation value. In our research the observation set is the output of the surmise module.

3) PARAMETER TRAINING AND ACTIVITY RECOGNITION

As mention above, the parameter set $\lambda = (\pi, A, B)$ of HMM module, is trained by Baum-Welch algorithm, which is a special case of the Expectation-Maximization algorithm (EM). It is an unsupervised algorithm running on the observation sequence input. The hidden states sequence which produces the observation sequence is unknown, so there is no need to input it. Initial HMM parameter estimation is given at very beginning, then the value of parameter is re-estimated by given data in order to reduce the error it may cause. In our context, this paper trains the model by adjusting and testing different floor situation to simulate real environment. The training process is given in equation 2.

Algorithm 2's input is collected data list *rae*, i.e. raw activity element. Every element in *rae* is the data of a complete walking. There are n hidden states; here n = 3, indicating three HMM parameters of λ. The 1st to 3rd line indicate creating and initializing algorithm data; the 4th line indicates denoising of raw data; the 5th to 9th indicate the DTW-KNN calculation and storage of result and data length; the 10th line indicates algorithm training using DTW-KNN data set and data length to generate the hidden states; the 11th line indicates the output of λ.

Algorithm 2 HMM Parameter Training

Input: Raw activity element list for training *rae*, Number of hidden states *n*
Output: parameters $\lambda = (\pi, A, B)$
1: *whole_data* = [];
2: *lengths* = [];
3: *data_size* = len(*rae*);
4: *wae* = wavelet(*rae*); // denoise the raw data
5: **for** w_i in *wae*:
6: fw_i = DTW_KNN(w_i);
7: l_i = len(fw_i);
8: *whole_data*.append(fw_i);
9: *lengths*.append(l_i);
10: λ = Baum-Welch(*whole_data*, *lengths*, *n*); //Baum-Welch has two parameters: training data set an data length
11: **return** λ;

After parameter training, then the HMM decision module is constructed. Viterbi algorithm is applied to recognize user gait. Using dynamic programming to find out the hidden state sequence of maximum probability, it is also called a Viterbi path. The recognition process is given in algorithm 3.

In the algorithm, the input is aq (raw activity queue) and ws (window size), and the output is the user status list tl. The first line declares a storage list, storing the inference value for a single recognition. The 2nd to 6th lines withdraw active elements cyclically from raw data and denoise them, then operate DTW-KNN algorithm and write in the storage list till recognition list satisfies the defined window size. The 7th to 8th data line identify the data in recognition list with Viterbi algorithm and return result.

Algorithm 3 Gait Recognition

Input: Raw activity element queue *aq*, Window size *ws*
Output: True status list *tl*
1: *cogList* = []
2: **while** len(*cogList*)< *ws*: // *add data in cogList to satisfy window size*
3: *rs* = *aq*.get();
4: *wrs* = wavelet(*rs*);
5: *cog* = DTW-KNN(*wrs*);
6: *cogList*.append(*cog*);
7: *tl* = Viterbi(*cogList*);
8: **return** *tl*

H. SYSTEM TIME COMPLEXITY ANALYSIS

A complete gait recognition is composed by different steps, including active element separation, selection, denoising, surmise and decision module. The average length of active element is given as *n*, and the complexity of each module is as follows.

Active element separation: from equation 1 and 3, the time complexity is

$$O\left(\frac{1}{N}n \cdot O(1)\right) + O(n \log n) + O(n) = O(n \log n) \quad (5)$$

Active element selection: as the sensors are small in number and fixed, so from algorithm 1 the time complexity is $O(1)$.

Denoising is based on wavelet transform and its complexity equals to the wavelet transform time complexity of $O(n \log n)$.

Predicting module: time complexity of DTW is $O(n^2)$, and that of KNN is based on one-sample dimension k and sample size m. Here $O(k \log m) = O(2 \log m) = O(\log m)$, and the total time complexity is $O\left(n^2\right) + O(\log m)$.

Decision module: as HMM adopts Viterbi algorithm for recognition, if the hidden state number is Q and the recognition window size is P, then the time complexity is $O(PQ^2)$. In summary, the whole system time complexity is $O(n \log n) + O(1) + O(n \log n) + O\left(n^2\right) + O(\log m) + O\left(PQ^2\right) = O\left(n^2\right) + O\left(PQ^2\right) + O(\log m)$. Yet in practice, Q and P are far less than *n*, and $O\left(PQ^2\right) \ll O\left(n^2\right)$. Here the value of m is fixed, so system time complexity is considered as $O\left(n^2\right)$, which meets the real time performance constraints.

IV. EXPERIMENTAL VERIFICATION

A. EXPERIMENTAL SETTINGS

Figure 4 depicts the experimental setup used in this investigation. The floor is made up of several 70*70 mm planks that have been joined together. As seen in Fig. 4-right, the backs of the planks are joined by metal dumpling chains. Each plank has five supporting feet: four at the corners and one in the middle. Not every adjacent board has a metal chain connecting it. A group of planks is made up of multiple planks, and Fig. 4's test floor is made up of various plank groups. Rather than connecting every adjacent plank to every other plank, dumpling chains are used to join a group of planks. One of the planks' supporting feet is elevated slightly to cause the planks to become unbalanced and mimic a loose floor.

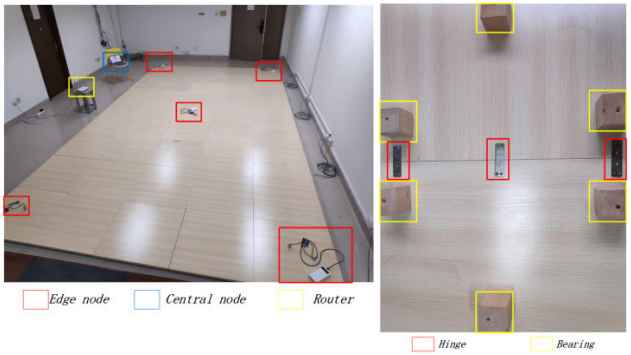

FIGURE 4. Experimental settings.

The center node is represented by the blue box in the upper left corner of Fig. 4, the router is represented by the yellow box, and the edge node is represented by the red box (see Fig. 3 for details). The edge nodes are dispersed throughout the four corners of the test area and the center region. There is at least one edge node for data collection associated with each group of planks. The center node manages the edge nodes via the SSH protocol to receive and store the activity components that are gathered, while the edge nodes communicate with each other via the WiFi network. Data can be safely transferred over unprotected networks using the encrypted network protocol SSH (Secure Shell). It offers a safe method for controlling and accessing computer systems from a distance. In the example, SSH protocol is used by the center node to control and interact with the edge nodes. Data is encrypted during transmission via SSH, preventing unauthorized users from accessing or altering the data's security and integrity. In order to ensure the safe operation of the entire system, the Secure Shell protocol enables the center node to securely receive, store, and manage the activity data acquired from the edge nodes. Considering that most indoor scenes are basically similar, compared to the experimental scenes in this article, although there are some external interference vibrations in the actual indoor scenes, they are different from human gait vibration signals and can be removed by simple denoising. Therefore, this article excludes these external interference vibrations to achieve the purpose of simplifying the experiment.

Two gait modes are designed in our experiment, one is NOR mode and the other is CRI mode. NOR simulates an average user who has no disease affecting his walk. CRI mode simulates a user with hemiplegia at the right leg. Each gait mode contains normal mode, abnormal mode and fall mode. The simulation method of the abnormal gait is that as one leg walks unsteadily with relaxing muscles while the other leg keeps the original walking pattern as possible. Meanwhile, due to the relatively singular gait of the elderly, this article only designed the two types of gaits mentioned above.

B. ACTIVE ELEMENTS CLASSIFICATION EXPERIMENT

To test the validity of our DTW-KNN framework, multiple indicators are compared with those in the Method of Characteristics [16], [20], which are chosen from time domain and frequency domain separately. Standard Deviation, entropy, peak value and partial signals before and after peak are chosen in the time domain; spectral centroid, peak position, peak amplitude, and power spectral density are selected in the frequency domain [15].

TABLE 1. DTW computation time and abnormal index variation rate in different segmentation.

Segment Sizes	400	350	300	250	200	150	100	50
Average computation time(s)	0.85	0.64	0.48	0.36	0.25	0.17	0.12	0.08
Abnormal index variation rate	0.00 %	0.35%	1.60%	2.70%	9.0%	10.50%	13.30 %	19.80%
Spatial variation rate	0.00 %	-19.70 %	-35.00%	-38.50%	-49.7%	-60.60%	-64.90 %	-63.70%

Table 1 shows the average time, change rate of abnormal index and spatial variation in related with segment sizes in one DTW calculation. In the experiment, there are 400 NOR mode normal active elements. The segment size refers to the number of samples for comparison each time. In a given segment size, the average computation time is the mean time spent to finish active element comparison in multiple tests. The change rate of abnormal index refers to the growth rate of DTW computation result compared to the direct calculation in a given segment size. Spatial variation rate is the growth rate of the space consumed in DTW compared with that in the direct calculation. As a single active element lasts less than 2 seconds, so the segment size 400 represents the situation of direct calculation.

From table 1, the average computation time is reduced as the segment size reducing, and the calculation speed is increased with a decreasing improving rate. Eventually, the ultimate recognition speed is 10 times faster than that in direct calculation. Moreover the abnormal index gradually increases, and dramatically increases when segment size is 300, 200 and 50, while change rate approaches to 20%. Also, the space consumed keeps decreasing constantly before

slightly increases when segment size is 50. Less than 50 (not listed in Table 1), computation speed demonstrates a modest increase while abnormal index has substantial increase, and the space consumed rises modestly too. Therefore, this paper chooses 50 as the segment size.

While the average computation time of the Method of Characteristics is 0.065 seconds, which is almost the same with DTW method; yet the space consumed is threefold to fourfold as much as the that of DTW. Therefore, the DTW computation is outperforming the Method of Characteristics.

Table 2 lists the related indicators when DTW and the Method of Characteristics are applied in SVM classifier and KNN classifier in both NOR and CRI gait mode. 70% of data are provided for training and 30% for testing, and the k value is 9. The results are analyzed in below.

TABLE 2. Training time comparison of two frameworks in CRI and NOR gait mode.

Gait Mode	Framework	Classifier	Accuracy	Precision	Recall Rate	F1	Aver. Trai. time (s)	Aver. Clas. time (s)
NOR	DTW	SVM	87.21%	86.02%	84.50%	86.38%	1.56	0.02
		KNN	91.54%	90.46%	89.74%	90.30%	0.15	0.09
	Method of Characteristics	SVM	73.25%	77.32%	74.56%	72.81%	35.78	0.07
		KNN	70.50%	71.64%	71.82%	70.31%	0.33	0.21
CRI	DTW	SVM	88.10%	85.82%	83.15%	84.19%	1.72	0.03
		KNN	90.34%	91.18%	90.56%	89.96%	0.17	0.08
	Method of Characteristics	SVM	55.44%	56.13%	55.74%	54.60%	34.97	0.07
		KNN	63.80%	64.29%	63.52%	62.21%	0.31	0.20

Here 200 normal active elements and 200 abnormal ones are used in the NOR mode. As to DTW, every indicator of KNN, except for the average classifying time, which is 0.07 seconds more than that of SVM, outperforms each indicator of SVM. As for the Method of Characteristics, however, every indicator of SVM outperforms that of KNN, except that SVM spends more training time than KNN. The SVM indicators using the Method of Characteristics perform 20% lower than the KNN indicators using DTW, caused by the result of wrongly classifying 40% to 50% abnormal active elements to normal. Yet such error would not possibly occurs in DTW-KNN. So it shows the absolute advantage of DTW-KNN compared with SVM using the Method of Characteristics.

Again, 200 normal active elements and 200 abnormal ones are used in the CRI mode. Table 2 explains that the DTW-KNN indicators perform mostly the same as those in NOR, while the indicators of SVM using the Method of Characteristics have dramatic decline in CRI than in NOR. So it indicates that DTW-KNN is able to adapt to different gait modes, yet SVM using the Method of Characteristics is not so.

As for the fall recognition, multiple fall active elements may be added in the KNN training data. The chance of misclassifying fall event is very low as the fall active element is distinctly different from other kind of element, so fall recognition is easy in the DTW-KNN model. Table 3 shows the testing results of NOR mode with fall active elements. Misclassification may happen as either normal elements are recognized as abnormal or vice versa; however none is recognized as fall element. Fall active elements are all correctly recognized.

TABLE 3. Confusion matrix with fall element.

Actual	Normal			Abnormal			Fall		
Classify	Normal	Abnormal	Fall	Normal	Abnormal	Fall	Normal	Abnormal	Fall
Counts	104	19	0	5	112	0	0	0	7

To summarize, the DTW-KNN framework is able to accurately classify various active elements of normal, abnormal and fall in different gait modes. However, this paper also uses HMM to identify gait mode when dealing with possible interference in actual environment.

C. GAIN RECOGNITION EXPERIMENT

In this experiment, there are two kinds of gaits, i.e. normal and abnormal. Normal gait indicates that user walks with set pattern, and abnormal gait indicates abnormal pattern.

TABLE 4. Comparison DTW-KNN indicators under steady/unsteady conditions.

window size	1	2	4	6	8
Accuracy	32%	93%	96%	95%	94%

The HMM identification accuracy rate varies with the change of the window size, as shown in table 4. The experimental data is the predicted sequence mixed with both NOR and CIR gait modes in the condition of stable experiment environment, i.e. the floor with no loose board. 70% of inference value in the predicted sequence is used for training and 30% for testing. Window size means the number of inference values of HMM recognition at one time. The accuracy rate is only 32% when the window size is 1, which is much lower than others; and when window size is 2, 4, 6 and 8, the accuracy rates are all above 93%, higher than that of surmise module. The peak value, which is 96%, appears when the window size is 4. After that, the accuracy rate shows slightly decrease as window size increases. Considering the issue of identification latency grows as window size increases, this paper sets the size as 4.

TABLE 5. HMM accuracy in different window size under steady condition.

DTW-KNN	Accuracy	Precision	Recall Rate	F1
NOR-stable	91.54%	90.46%	89.74%	90.30%
NOR-unstable	85.19%	86.64%	85.67%	85.4%
CRI-stable	90.34%	91.18%	90.56%	89.96%
CRI-unstable	82.18%	83.73%	82.51%	82.94%

Table 5 shows the comparison of indicators in the surmise module when two gait modes appear in different experiment environments, stable and unstable. In unstable environment, there are 15% of loose floorboards, distributed as equally as possible. Under this condition, table 5 shows that the indicator's performance of NOR mode have declined by about 5% and those of CRI mode have declined by 8%. In summary, it show a pattern of regularity that if a certain active element is influenced by loose floorboards, then the inference values of successive three elements, including the previous one, will be affected. Considering this pattern, HMM is able to improve the identification accuracy rate.

In figure 5 this paper compares the accuracy rates in the surmise module and HMM in the four combinations of gait modes and environments. From this figure, the accuracy rate increased by 5% to 12% when using HMM. Moreover, most inference errors happen in the CRI-Unstable combination, and the accuracy rate of HMM in this situation is still as much as 94%. Correction rates in different combination are also given in this figure. This is a new indicator defined as the HMM correction inference value divided by the error inference value. This indicator measures the ability of HMM correcting the interfered active elements, and the higher the correction rate, the more robust and adaptive the HMM could be. In all combinations, HMM shows good correction performance at an average level of 88.75%. HMM is helpful in increasing the overall performance of systematic identification rate, and hence improving the systematic robustness.

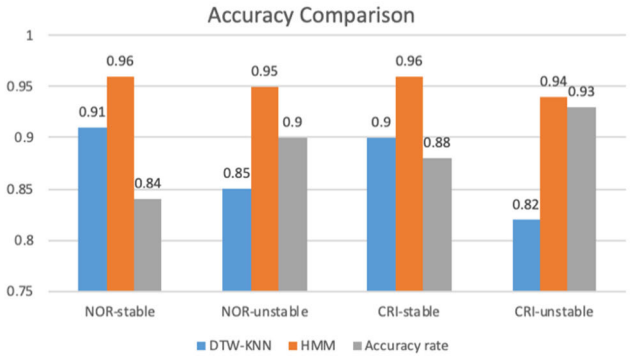

FIGURE 5. Accuracy comparison of DTW-KNN vs. HMM.

V. CONCLUSION

This paper studies the detection of abnormal gait identification based on vibration signals, which has been little studied. Vibration signals are acquired, and we calculate inference value of active element by the improved DTW-KNN framework. This method shows better adaptivity for different gait modes, hence solving the problem that the Method of Characteristics has difficulty to identify correct feature of different gait modes. The predicted sequence is further analyzed by HMM to correct the inference value effected by uncontrolled interferences. The experimental results show that the method can effectively identify abnormal gait and the recognition accuracy rate reaches 95.25%, and the correction performance is as good as 88.75%. Through experiments, it can be seen that the specific contribution of this paper is to cope with the recognition difficulty caused by the diversity of gaits by comparing various gaits; HMM algorithm is used to reduce the impact of environmental interference. Adapt to changes by quickly collecting data for training.

Future studies will optimize this method by addressing the following aspects:

(1) For users who are using crutches or other walking assistance, we currently analyze their gait pattern by only considering walking with legs. To accommodate there users better, more adaptable techniques should be developed. For example, creating a detection system that identifies the number of actives in a cycle during training would be beneficial.

(2) The distributed architecture of the vibration signal system is not fully utilized. To address this, a dialogue mechanism enabling nodes to communicate, independently selecting the center and activity element for load balancing should be incorporated into the system.

APPENDIX

Abbreviation	Whole Phrase
DTW	Dynamic Time Warping
KNN	K-Nearest Neighbor
HMM	Hidden Markov Model
IOT	Internet of Things
FFT	Fast Fourier Transform
NTP	Network Time Protocol
SVM	Support Vector Machine

REFERENCES

[1] (2021). *The 7th National Population Census of China*. [Online]. Available: http://www.bookref.com

[2] (2023). *United Nations World Social Report*. [Online]. Available: https://desapublications.un.org/publications/world-social-report-2023-leaving-no-one-behind-ageing-world

[3] C. Wang, C. Zhen, and Z. Zen, "Sleep movement recognition based on software-defined intelligence," *Chin. J. Electron.*, vol. 49, no. 1, pp. 85–89, 2021.

[4] B. Saha, M. S. Islam, A. K. Riad, S. Tahora, H. Shahriar, and S. Sneha, "BlockTheFall: Wearable device-based fall detection framework powered by machine learning and blockchain for elderly care," in *Proc. IEEE 47th Annu. Comput., Softw., Appl. Conf. (COMPSAC)*, Jun. 2023, pp. 1412–1417.

[5] X. Wang, D. Ristic-Durrant, M. Spranger, and A. Gräser, "Gait assessment system based on novel gait variability measures," in *Proc. Int. Conf. Rehabil. Robot. (ICORR)*, Jul. 2017, pp. 467–472.

[6] Z. Ni and B. Huang, "Gait-based person identification and intruder detection using mm-wave sensing in multi-person scenario," *IEEE Sensors J.*, vol. 22, no. 10, pp. 9713–9723, May 2022.

[7] S. He, K. Xie, W. Chen, D. Zhang, and J. Wen, "Energy-aware routing for SWIPT in multi-hop energy-constrained wireless network," *IEEE Access*, vol. 6, pp. 17996–18008, 2018.

[8] L. Yao, W. Kusakunniran, Q. Wu, J. Zhang, and Z. Tang, "Robust CNN-based gait verification and identification using skeleton gait energy image," in *Proc. Digit. Image Comput., Techn. Appl. (DICTA)*, Dec. 2018, pp. 1–7.

[9] M. Babaee, L. Li, and G. Rigoll, "Gait recognition from incomplete gait cycle," in *Proc. 25th IEEE Int. Conf. Image Process. (ICIP)*, Oct. 2018, pp. 768–772.

[10] T.-N. Nguyen, H.-H. Huynh, and J. Meunier, "Skeleton-based abnormal gait detection," *Sensors*, vol. 16, no. 11, p. 1792, Oct. 2016.
[11] H. Zhang and C. Ye, "An RGB-D camera based walking pattern recognition by support vector machines for a smart rollator," *Int. J. Intell. Robot. Appl.*, vol. 1, no. 1, pp. 32–41, 2017.
[12] R. Liao, C. Cao, and E. Garcia, "Pose-based temporal–spatial network (PTSN) for gait recognition with carrying and clothing variations," in *Proc. Chin. Conf. Biometric Recognit.*, 2017, pp 474–483.
[13] C. A. Ronao and S.-B. Cho, "Recognizing human activities from smartphone sensors using hierarchical continuous hidden Markov models," *Int. J. Distrib. Sensor Netw.*, vol. 13, no. 1, Jan. 2017, Art. no. 155014771668368.
[14] R. San-Segundo, H. Blunck, J. Moreno-Pimentel, A. Stisen, and M. Gil-Martín, "Robust human activity recognition using smartwatches and smartphones," *Eng. Appl. Artif. Intell.*, vol. 72, pp. 190–202, Jun. 2018.
[15] F. Lin, A. Wang, Y. Zhuang, M. R. Tomita, and W. Xu, "Smart insole: A wearable sensor device for unobtrusive gait monitoring in daily life," *IEEE Trans. Ind. Informat.*, vol. 12, no. 6, pp. 2281–2291, Dec. 2016.
[16] Y. Dong, J. Zhu, and H. Y. Noh, "Re-vibe: Vibration-based indoor person re-identification through cross-structure optimal transport," in *Proc. 9th ACM Int. Conf. Syst. Energy-Efficient Buildings, Cities, Transp.*, Nov. 2022, pp. 348–352.
[17] J. Clemente, W. Song, M. Valero, F. Li, and X. Liy, "Indoor person identification and fall detection through non-intrusive floor seismic sensing," in *Proc. IEEE Int. Conf. Smart Comput. (SMARTCOMP)*, Jun. 2019, pp. 417–424.
[18] S. Pan, T. Yu, and M. Mirshekari, "FootprintID: Indoor pedestrian identification through ambient structural vibration sensing," *ACM Interact. Mob. Wearable Ubiquitous Technol.*, vol. 1, no. 3, pp. 1–89, 2017.
[19] R. Bono, "Transducer mounting and test setup configurations," in *Proc. IMAC 26th Tutorial. Sem*, 2008, pp. 1–45.
[20] J. Clemente, F. Li, M. Valero, and W. Song, "Smart seismic sensing for indoor fall detection, location, and notification," *IEEE J. Biomed. Health Informat.*, vol. 24, no. 2, pp. 524–532, Feb. 2020.

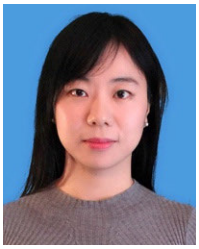

JUANJUAN CHEN was born in Sichuan, China, in 1980. She received the B.S. degree in industrial foreign trade and the M.S. degree in supply chain management from Chongqing University, China.

Currently, she is a Senior Lecturer teaching with the School of Computer and Information Science, Chongqing Normal University. She has published eight academic articles indexed by SCI or EI and two inventive patents. Her major research interest includes teaching and research in computer application technology.

CHENGLIANG WANG (Member, IEEE) was born in Guizhou, China, in 1975. He received the B.S. degree in mechatronics, the M.S. degree in precision instruments and machinery, and the Ph.D. degree in control theory and control engineering from Chongqing University.

Currently, he is a Professor been long engaged in artificial intelligence theory and application, teaching and research in computer application technology. He is also a Principal Lecturer and a Scientist with the College of Computer Science, a Postgraduate Students Supervisor, and a fellow of Chinese Computer Federation. He has published more than 80 academic articles indexed in key journals, which are indexed by SCI or EI. He holds 22 inventive patents and also innovated and actively participating more than nine national projects. His research interests include complex system intelligent processing and artificial intelligence theory and application.

Prof. Wang is the fellow of Chinese Computer Federation.

YILUO LIU was born in Chongqing, China, in 1996. He received the B.S. degree in computer science and technology from Chongqing University, China, in 2019, where he is currently pursuing the master's degree in computer science and technology with the College of Computer Science.

His current research interests include signal processing and machine learning.